Texture of tetragonal α-$FeSi_2$ films on Si(001)

C. Detavernier,* C. Lavoie, and J. Jordan-Sweet
IBM T. J. Watson Research Center, Yorktown Heights, New York 10598, USA

A. S. Özcan
Department of Physics, Boston University, Boston, Massachusetts 02215, USA
(Received 6 November 2003; published 21 May 2004)

Synchrotron radiation was used to measure pole figures of α-$FeSi_2$ films on Si(001) substrates. The pole figures consist of complex, though symmetrical patterns of narrow lines. These lines are indicative of axiotaxy, a peculiar type of preferential orientation which has been recently reported to occur in NiSi films on Si(001). The patterns of lines are created by grains for which the α-$FeSi_2$(110) or (102)-type planes are parallel to Si(110)-type planes in the substrate. As a direct consequence of the constraint that a set of planes in the film is aligned to a set of planes in the substrate, the texture manifests itself as though it were a fiber texture, with the fiber axis normal to the Si(110)-type planes (i.e., at 45° and 90° from the surface normal). The spacing of 1.905 Å between α-$FeSi_2$(110) planes is almost identical to the spacing of 1.920 Å between Si(220) planes. Hence, if α-$FeSi_2$(110)-type planes are parallel to Si(110)-type planes, the resulting interface with the Si(001) substrate is periodic along the Si(100)-type directions in the plane of the interface. The brightest spots along the lines are caused by grains which are epitaxially aligned with the Si substrate. In addition to the axiotaxy, four different types of epitaxial texture components could be identified within the same film.

DOI: 10.1103/PhysRevB.69.174106 PACS number(s): 68.55.Jk

I. INTRODUCTION

Texture is an important characteristic of the microstructure of polycrystalline materials.[1–4] Although x-ray diffraction (XRD) and orientation imaging microscopy (OIM) are used routinely for bulk samples, texture measurement for thin films is more challenging.[5–7] OIM is difficult because of the small grain size typically encountered in thin film samples, while XRD is time consuming due to the limited intensity of lab-based x-ray sources. However, new techniques have provided ways of measuring texture in a more efficient way. A first method is to use a lab-based x-ray source, but limit the time necessary to measure a pole figure by using an area detector to measure the intensity variation along the Debye rings. Software allows the user to determine the complete orientation density function of a given sample. A second approach, which was used for the measurements in this paper, consists of using a standard detector and measurement geometry, while benefiting from the high x-ray intensity available at a synchrotron to increase the acquisition speed and to increase the level of detail that can be observed in a pole figure by using small steps in both χ and ϕ during the measurement.

The pole figure for a certain (hkl) plane represents the statistical distribution of the orientation of the normal to this plane. One can imagine that the sample is positioned in the center of a hemisphere (Fig. 1). The angles ϕ and χ are standard spherical coordinates (i.e., azimuth and elevation), with $\chi=0°$ for the normal to the substrate and $\chi=90°$ for directions parallel to the surface of the sample. For each grain in the film, one can mark the intersection between the normal to the (hkl) plane within that grain and the hemisphere. Different shades of gray on the surface of the hemisphere represent the areal density of these intersection points, with black indicating the regions with highest diffracted intensity. The pole figure for the (hkl) plane is formed by projecting the image from the hemisphere onto a flat surface. The creation of the α-$FeSi_2$(110) pole figure using an orthogonal projection is illustrated in Fig. 1.

Texture in thin films is usually classified into three of the following categories. For a random texture, the grains in the film form an ideal powder, and there is a homogeneous diffracted intensity across the whole pole figure. For a fiber texture, the grains in the film are oriented in such a way that a given plane is preferentially parallel to the surface of the film, while there is a degree of freedom for rotation around the fiber axis (i.e., around the surface normal).[6] A fiber texture is easily identified by XRD: measurements in a standard

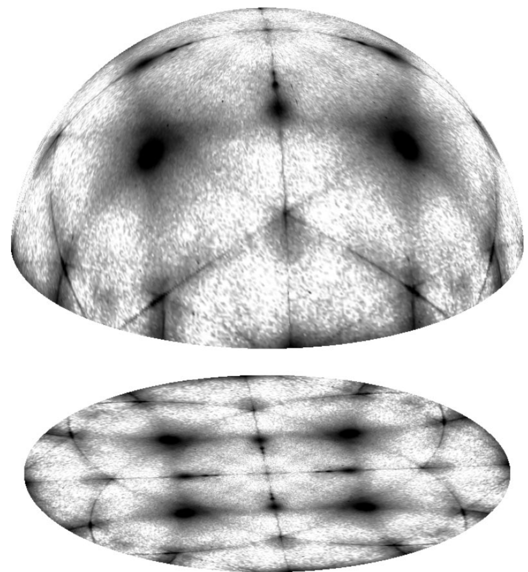

FIG. 1. An example showing the projection used to obtain the α-$FeSi_2$(110) pole figure.

 ©2004 The American Physical Society

$\theta/2\theta$ geometry will show a very strong diffraction peak for the plane that is parallel to the surface of the film, while pole figures for other planes will exhibit circular rings, centered around the middle of the pole figure. A third category is epitaxial alignment (or in-plane texture), for which the orientation of the grain is completely fixed with respect to the crystallographic axes of the single-crystalline substrate. For epitaxial films, XRD measurements in a standard $\theta/2\theta$ geometry will show a very strong diffraction peak for the plane that is parallel to the surface of the film, while pole figures for other planes will show spots of high diffracted intensity.

Recently, a new type of texture has been observed in thin NiSi films on Si(001), which was named "axiotaxy."[8] Although the crystal structure of orthorhombic NiSi is very different from the cubic diamond structure of silicon, certain low index planes exist within the NiSi lattice for which the d spacing is almost identical to the spacing between Si(220)-type planes in the substrate. Because of the excellent match in d spacing, these lattice planes in the NiSi film were observed to be preferentially aligned parallel to the Si(220)-type planes in the substrate. In contrast to epitaxy, which is characterized by good matching within the plane of the interface, axiotaxy involves the alignment of planes across the interface. The occurrence of axiotaxy can be identified by the presence of complex, though symmetrical patterns of lines on the pole figures.

Silicides are metal-silicon compounds. Thin silicide films are frequently formed by a solid-state reaction between a deposited metal film and a single crystal Si substrate. Although a lot of work has been reported on "epitaxial" films (e.g., $NiSi_2$, $CoSi_2$, β-$FeSi_2$, rare-earth silicides, etc.), only a handful of papers include extensive texture measurements.[8–11] In view of possible applications in optoelectronics, a lot of effort has been devoted to growing epitaxial layers of semiconductive β-$FeSi_2$ on Si substrates.[12,13] It is known from this work that tetragonal α-$FeSi_2$ and several metastable phases (e.g., cubic CsCl- and CaF_2-type structures) can grow epitaxially on Si substrates.[14,15] Most of the experimental work in this field was done using molecular-beam epitaxy, with the intent of forming "perfect" epitaxial silicides.

In this paper we investigate the texture of α-$FeSi_2$ thin films on Si(001) substrates utilizing high-resolution, synchrotron based x-ray pole figure analysis. Instead of trying to optimize the growth process, we deposited a relatively thick film of Fe on a Si(001) substrate, and heated it in order to form $FeSi_2$.

II. EXPERIMENT

A 30 nm thick Fe film was sputter deposited onto a Si(100) substrate that was cleaned in a hydrogen fluoride solution. α-$FeSi_2$ was formed by annealing the sample for 30 s at 950 °C in Ar. The XRD measurements were performed at the X20A beamline of the National Synchrotron Light Source (NSLS) in Brookhaven National Laboratory. A Si monochromator was used to select a wavelength of 1.54 Å. This wavelength was chosen to simplify comparison with lab-based measurements using Cu $K\alpha$ radiation. The sample was mounted on a four-circle diffractometer (Schultz geometry). We used a scintillation counter to detect the diffracted intensity. The pole figures were acquired in steps of 0.5° in ϕ and χ ($0\leqslant\phi\leqslant 90°$ and $0\leqslant\chi\leqslant 85°$). The sample was aligned by setting ϕ and χ equal to 45° at the location of the Si(011) substrate peak. As a consequence, the directions ($\phi=0°$, $\chi=0°$), ($\phi=0°$, $\chi=90°$), and ($\phi=90°$, $\chi=90°$) correspond to the Si(0,0,1), Si(-1,1,0) and Si(1,1,0) poles, respectively. The location of other low-index substrate poles for this alignment is indicated in Fig. 2. Because of geometrical effects, the background within a pole figure changes as a function of χ. The shape of the background was determined by measuring χ scans for $\theta/2\theta$ values positioned just next to the diffraction peak for which the pole figure was measured. When subtracting the background for an (hkl) pole figure in this way, the intensity of the point at ($\phi=0°$, $\chi=0°$) was set equal to the intensity of the (hkl) peak in a standard $\theta/2\theta$ scan.

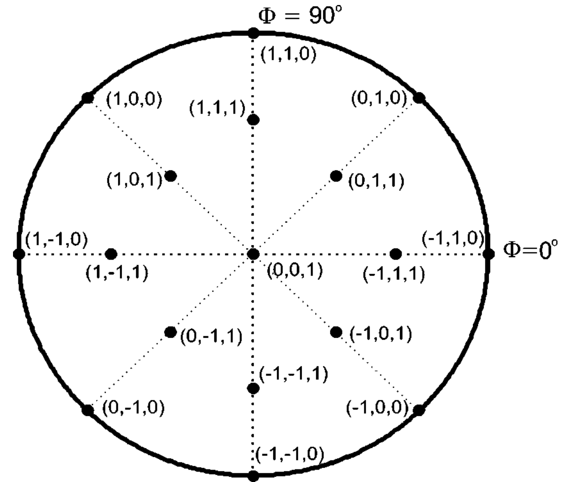

FIG. 2. The location of low-index poles of the Si substrate for the sample alignment used in this paper. The Si(110)-type cleaving directions are at $\phi=0°$ and 90°.

III. RESULTS

A. XRD scans in Bragg-Brentano geometry

The presence of a single phase of tetragonal α-$FeSi_2$ [$a=b=2.6939$ Å, $c=5.1361$ Å (Ref. 16)] was verified using a standard $\theta/2\theta$ XRD scan in the Bragg-Brentano geometry (Fig. 3). Peak fitting results in positions and relative intensities. The measured peak positions correspond reasonably well to the values from the JCPDS database.[16] Fiber texture or epitaxial alignment can be easily recognized from a standard $\theta/2\theta$ scan, since both types of texture result in a certain crystallographic plane of the film to be preferentially oriented parallel to the surface. As a consequence, the XRD peak that is generated by diffraction from this plane will have a very high intensity. In the case of a strongly textured film, no other diffraction peaks will be observed. The presence of various diffraction peaks in Fig. 3 seems to indicate that there is no strong preferential orientation of the grains in the layer. However, the intensity ratios of the various peaks do not agree with the expected values for a powder sample (Table I).

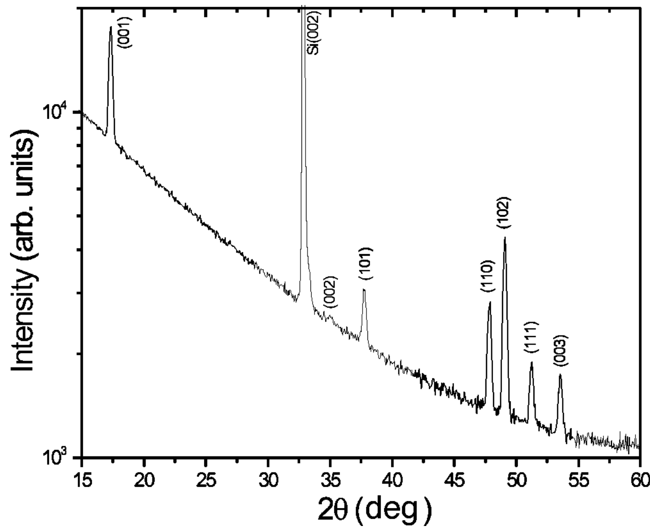

FIG. 3. $\theta/2\theta$ XRD measurement for an α-$FeSi_2$ film on a Si(001) substrate. The peaks are indexed according to tetragonal α-$FeSi_2$ (see Table I).

B. Pole figures

The (101), (110), and (102) pole figures for α-$FeSi_2$ films on Si(001) are shown in Figs. 4–6. These (hkl) planes were selected for pole figure measurements because the corresponding diffraction peaks are intense and separated by at least 1° in 2θ from neighboring XRD peaks. The presence of complex, though symmetrical patterns of lines on the pole figures is intriguing, and suggests that the texture of α-$FeSi_2$ films cannot be categorized within the standard classification of random, fiber texture and epitaxial alignment mentioned in the Introduction. When plotting the (101) pole figure on a spherical surface, it is clear that the line patterns in the planar pole figure actually correspond to circles on a sphere (Fig. 7). These circles are similar to the circles that are expected for a fiber texture. In this case, the fiber axes are located at $(\chi=45°;\phi=45°,135°,225°,315°)$ and $(\chi=90°;\phi=0°, 90°,180°,270°)$, instead of at $\chi=0°$ (i.e., normal to the surface of the sample) as expected for a standard fiber texture. According to Fig. 2, the fiber axes are pointing in directions parallel to Si(110)-type poles from the substrate. We will henceforth use the notation $\langle hkl \rangle$ to indicate a family of planes, i.e., Si$\langle 110 \rangle$ refers to a set of planes (and poles) including Si(110), Si(101), Si(-110), etc. The angle between the fiber axis and a point on the corresponding circle on the (101) pole figure is 51°, which corresponds to the angle between the (101) and (110) planes in the tetragonal α-$FeSi_2$ lattice. One can conclude from this that the linear features on the (101) pole figure are created by a fiberlike texture, with the α-$FeSi_2\langle 110 \rangle$ fiber axis parallel to Si$\langle 110 \rangle$. This understanding of the origin of the lines on the pole figures was then employed to calculate the patterns for the other pole figures (Figs. 4–6). These calculations should not be considered as "fitting," since no adjustable parameters are involved. Indeed, for a given orientation of the fiber axis [which can be determined from the three-dimensional (3D) representation of the data as shown in Fig. 7], the position of the lines in the planar representation of the pole figure is completely determined by geometry.

The most intense lines on the pole figures are created by the diffraction from grains for which α-$FeSi_2\langle 110 \rangle$ is parallel to Si$\langle 110 \rangle$. The $\langle 110 \rangle$ fiber axes are expected to result in spots of high diffracted intensity at $\chi=45°$ and $\phi=45°,135°,225°,315°$ on the (110) pole figure. This can be observed in Fig. 5, although part of the intensity that is observed at these locations is related to contamination from the neighboring Si(220) peak.

When carefully studying the pole figures, one can observe another set of lines, which are not as intense, but nevertheless clearly visible. This second set of lines is created by a group of grains for which α-$FeSi_2\langle 102 \rangle$ is parallel to Si$\langle 110 \rangle$. It should be noted that since the a and b axes have the same length in the tetragonal structure, the (102) and (012) planes are equivalent.

In summary, the line patterns on the pole figures are generated because of the preferred alignment of α-$FeSi_2\langle 110 \rangle$ and $\langle 102 \rangle$ planes parallel to Si$\langle 110 \rangle$. The constraint that one set of planes in the film is parallel to a set of planes in the substrate generates a fiberlike texture, with the fiber axis perpendicular to Si$\langle 110 \rangle$. The lines on the pole figure are in fact circles on a spherical surface, around fiber axes located at (χ=45°; ϕ=45°,135°,225°,315°) and (χ=90°; ϕ=0°,90°,180°,270°). The excellent fit that was obtained between the calculated patterns and the measured pole figures indicates that this model provides a good understanding of the crystallographic orientation of the grains that are responsible for the line patterns.

TABLE I. Crystallographic data for tetragonal [α-$FeSi_2$ [$a=b=2.6939$ Å, $c=5.1361$ Å] (Ref. 16)]. The theoretically expected peak positions and intensities for a powder sample (according to the JCPDS database) are compared with the experimentally determined peak intensities for a film on a Si(001) substrate.

hkl	2θ(°) Measured	2θ(°) JCPDS	d(Å) JCPDS	I JCPDS	I Si(001)
001	17.31	17.252	5.1358	390	1000
101	37.76	37.667	2.3861	590	98
110	47.83	47.711	1.9046	510	157
102	49.10	48.968	1.8586	1000	313
111	51.23	51.123	1.7852	120	64
003	53.57	53.470	1.7122	110	54

C. Axiotaxy

The remaining question regards the physical mechanism that is responsible for this peculiar preferential alignment of the tetragonal $FeSi_2$ lattice with respect to the cubic Si lattice. Known driving forces for texture formation include the minimization of surface, interface or strain energy. These driving forces are typically used to explain why a certain crystallographic plane of the film is preferentially parallel to the surface and interface. This approach works for standard fiber texture and epitaxy, since both of these cases are characterized by a single (hkl) plane that is parallel to the sur-

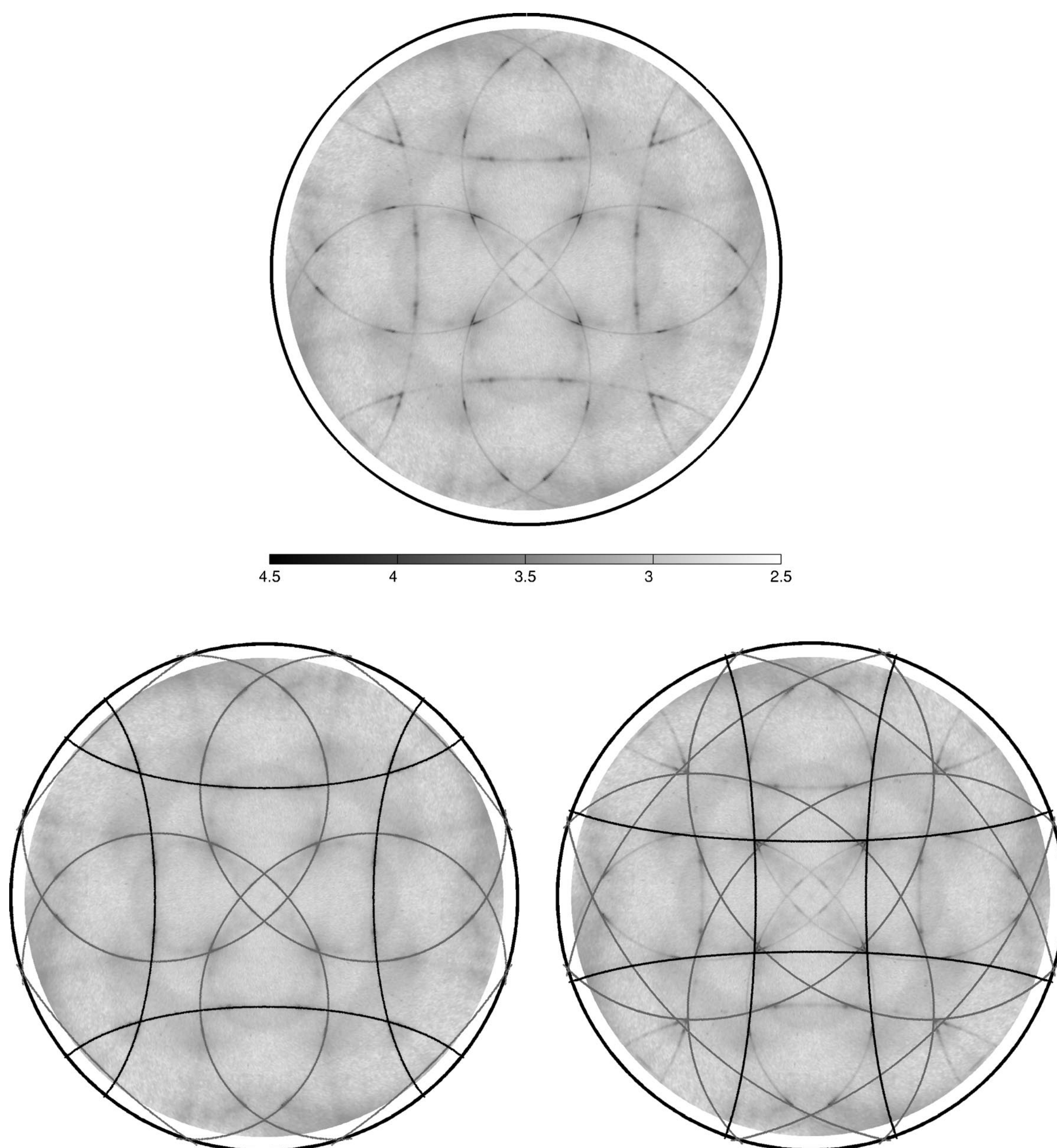

FIG. 4. The (101) pole figure. The data are shown as measured (top figure), and with fitting results overlaid on top of the measured data. The grayscale indicates the diffracted intensity, expressed on a logarithmic scale. The calculations assume that α-$FeSi_2\langle 110\rangle$ (bottom left) or $\langle 102\rangle$ (bottom right) is parallel to Si$\langle 110\rangle$. The line patterns shown in gray are calculated for the fiber axes at (χ=45°;ϕ=45°,135°, 225°,315°), while the line patterns in black were calculated for the fiber axes located at (χ=90°;ϕ=0°,90°,180°,270°).

face and interface. However, for the present case of off-normal fiber texture, the fact that the fiber axis is not normal to the substrate causes different crystallographic planes to be parallel to the surface and interface of the film for each degree of rotation around the fiber axis.

An important indication is provided by comparing the spacing between the "aligned" planes in the film and the substrate. According to Table I, the spacing between α-$FeSi_2$ (110) planes is 1.9046 Å, a value which differs by only 0.81% from the spacing of 1.9201 Å between Si(220) planes. When taking into account the difference in thermal-expansion coefficient between α-$FeSi_2$ and Si (7.7 versus 2.6 ppm/K, respectively), one can expect this difference to become even smaller at higher temperature. Indeed, according to Fig. 8, the difference becomes only 0.03% at 800 °C, which is near the temperature at which the α-$FeSi_2$ is formed during the solid-state reaction.

If the α-$FeSi_2\langle 110\rangle$ planes are parallel to the Si$\langle 110\rangle$ planes in the substrate, the resulting interface with the Si(001) substrate will be periodic along the Si$\langle 100\rangle$ directions in the plane of the interface, as illustrated schematically in Fig. 9. In the case of epitaxial alignment, there is a good match between the atomic positions in film and substrate at the interface, and a periodic interface structure is formed in two dimensions. In the present case, a periodic structure is only formed in one dimension (i.e., in the direction along the

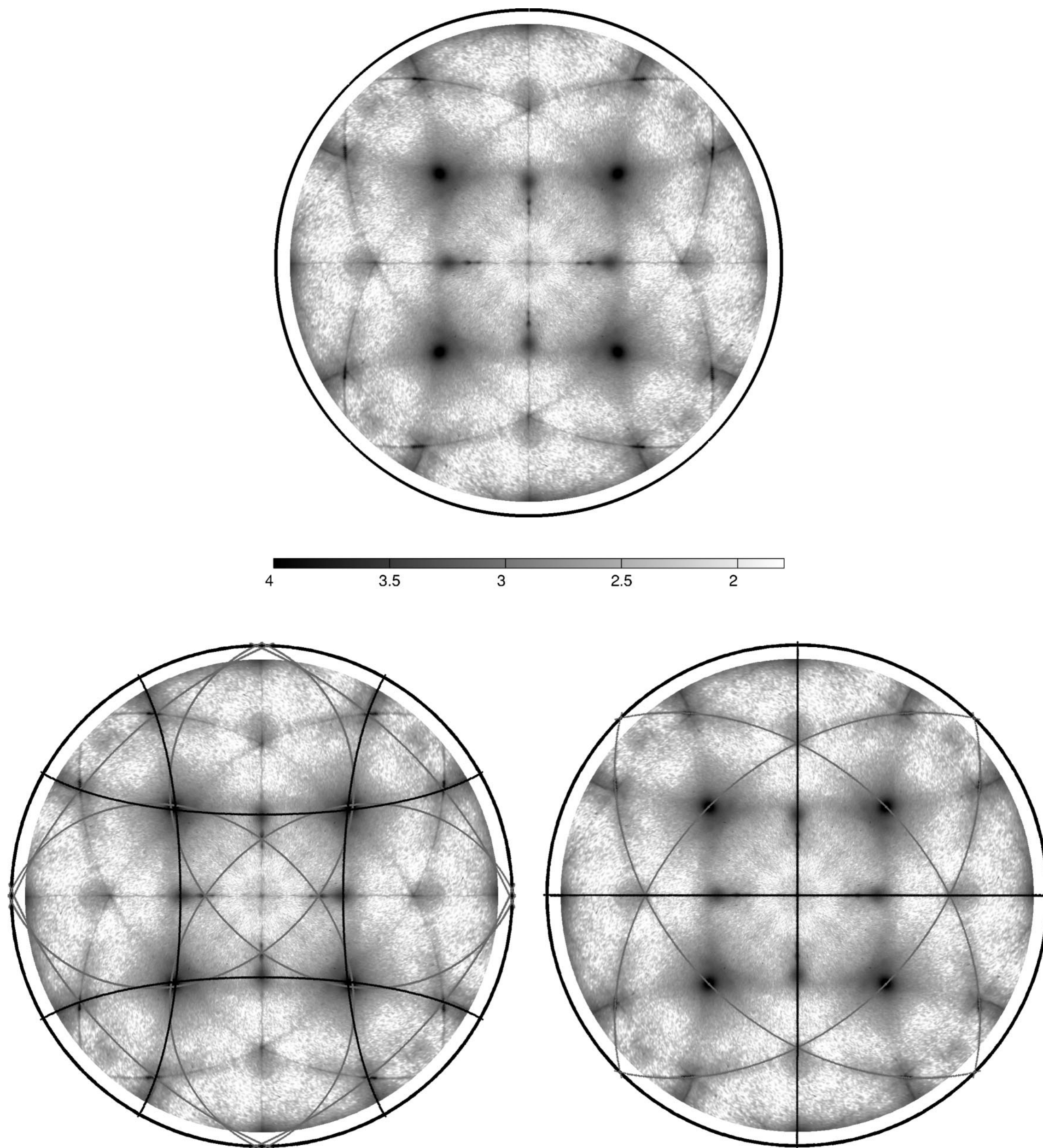

FIG. 5. The (110) pole figure. The data are shown as measured (top figure), and with fitting results overlaid on top of the measured data. The grayscale indicates the diffracted intensity, expressed on a logarithmic scale. The calculations assume that α-$FeSi_2\langle 110\rangle$ (bottom left) or $\langle 102\rangle$ (bottom right) is parallel to Si$\langle 110\rangle$. The line patterns shown in gray are calculated for the fiber axes at ($\chi=45°;\phi=45°,135°,225°,315°$), while the line patterns in black were calculated for the fiber axes located at ($\chi=90°;\phi=0°,90°,180°,270°$).

interface that is found by projecting the apparent fiber axis onto the interface plane). In view of this periodicity along one direction or axis, the term axiotaxy was proposed in a previous paper.[8] The 1D periodicity in the plane of the interface for axiotaxy can be considered as an intermediate case between the 2D periodicity for epitaxial alignment and no periodicity for a random interface.

It should be noted that although the idea of alignment of planes in the film and substrate that share the same d spacing can be used to explain the observed patterns in the pole figures, it cannot be used as such to unambiguously predict the occurrence of axiotaxy for any given film/substrate combination. One could naively assume that plane alignment will always occur whenever a low-index plane in the film has the same d spacing as a low-index plane in the substrate. However, when comparing the d spacings of low-index planes in α-$FeSi_2$ and Si, one finds that there is not only an excellent match in d spacing between the α-$FeSi_2(110)$ and Si(220) plane (which was used to explain the experimentally observed patterns), but also between α-$FeSi_2(200)$ and Si(400). Indeed, the difference in d spacing between the latter two planes is only 0.03% at 800 °C. However, no axiotaxy was experimentally observed with a fiber axis along Si$\langle 100\rangle$ poles. Although alignment with Si$\langle 100\rangle$ is geometrically possible, plane alignment with Si$\langle 110\rangle$ planes appears to be preferred. One possible explanation is related to the covalent

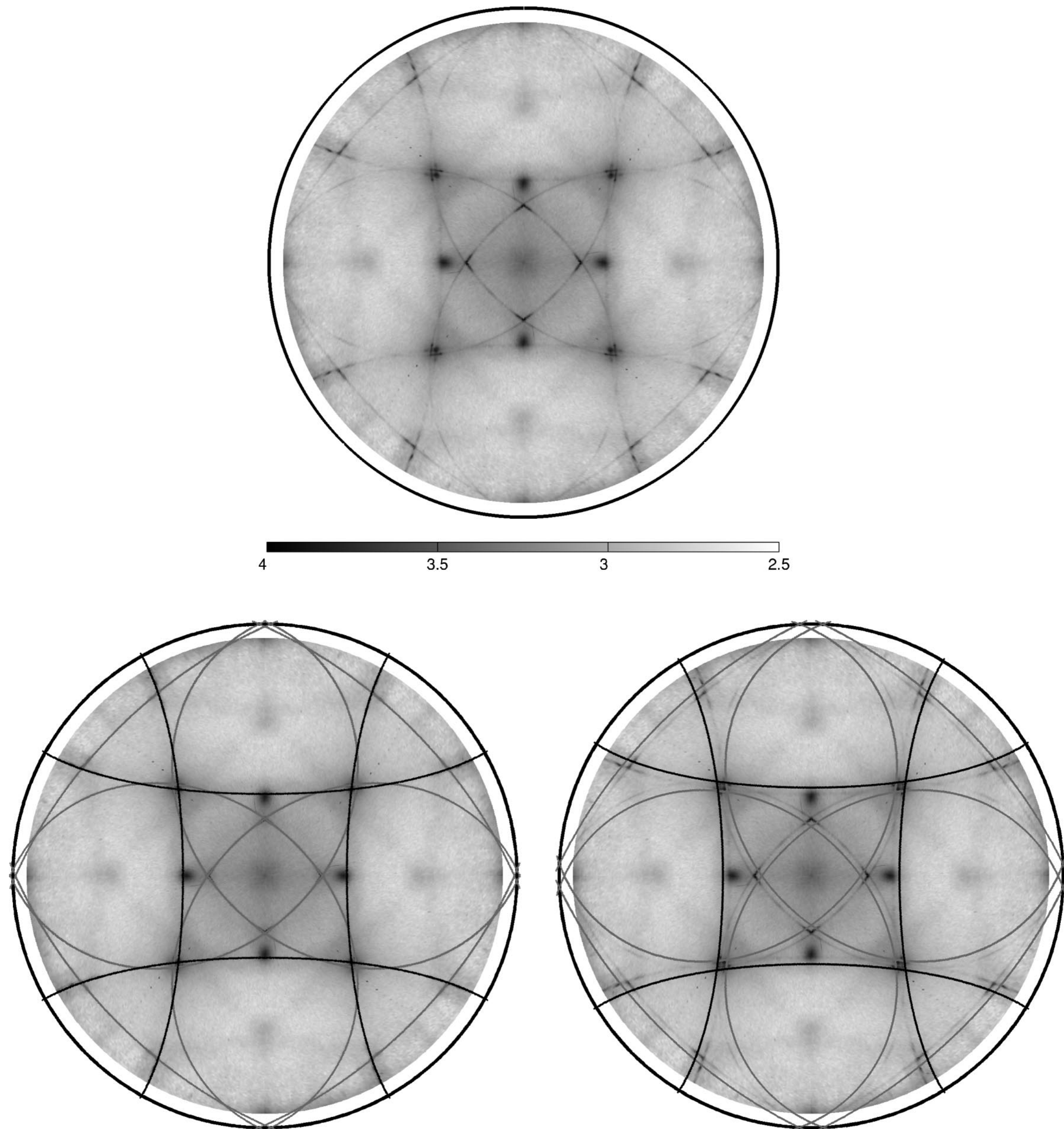

FIG. 6. The (102) pole figure. The data are shown as measured (top figure), and with fitting results overlaid on top of the measured data. The grayscale indicates the diffracted intensity, expressed on a logarithmic scale. The calculations assume that α-$FeSi_2\langle 110\rangle$ (bottom left) or $\langle 102\rangle$ (bottom right) is parallel to Si$\langle 110\rangle$. The line patterns shown in gray are calculated for the fiber axes at ($\chi=45°;\phi=45°,135°,225°,315°$), while the line patterns in black were calculated for the fiber axes located at ($\chi=90°;\phi=0°,90°,180°,270°$).

bonding in the Si substrate. Since the bonds in Si are along (111) directions (i.e., perpendicular to Si$\langle 111\rangle$ planes), two of the four bonds per atom are within a Si$\langle 110\rangle$ plane, while the other two bonds make an angle of 54.74° with the Si$\langle 110\rangle$ plane. None of the covalent bonds are within Si$\langle 100\rangle$ planes. It could be argued that alignment with Si$\langle 110\rangle$ planes is energetically favored, since this allows for improved bonding geometry at the interface. However, further research is needed to unambiguously identify the selection mechanism, since a kinetics-based mechanism (e.g., growth anisotropy during phase formation) cannot be ruled out at this point.

D. Axiotaxy versus epitaxy

A final question that arises regarding the intensity variation along the lines. Indeed, since the grayscale on the pole figures is logarithmic, there are significant differences in diffracted intensity between points on the same line.

When positioning a grain, there are three degrees of freedom for orientation. The axiotaxy fixes the orientation of $FeSi_2\langle 110\rangle$ parallel to Si$\langle 110\rangle$ (e.g., at $\chi=45°$, $\phi=45°$). Fixing the χ and ϕ angle for one plane in the grain provides a constraint which leaves a single degree of freedom (i.e., rotation around the fiber axis), creating one-dimensional features on the pole figures. Choosing a second constraint by

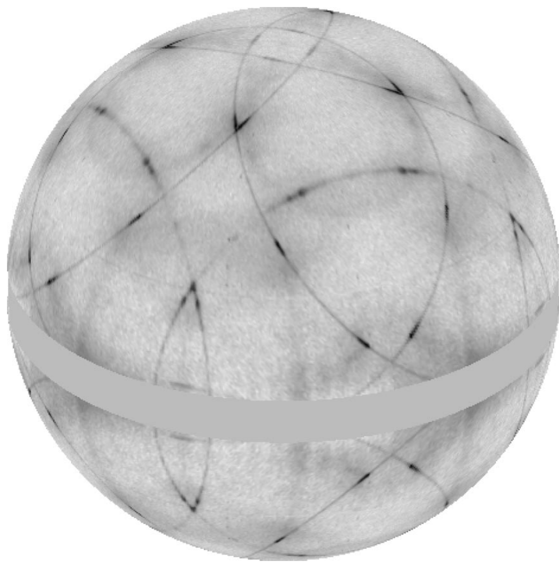

FIG. 7. The (101) pole figure as an intensity chart overlayed on top of a unit sphere. The equatorial band with uniform intensity is the region between $85<\chi\leqslant 95°$, for which no measured values were available.

selecting a point on one of these lines results in a situation with zero remaining degrees of freedom, i.e., the orientation of the grain is completely defined. The high intensity spotlike features on the lines can therefore be considered as a standard in-plane texture (sometimes also referred to as epitaxial alignment), for which the orientation of the grain is completely fixed with respect to the single-crystal substrate.

The high-intensity points on the lines on the pole figures are generated by four different types of epitaxial alignment: (1) $FeSi_2$(001)//Si(001) and $FeSi_2$(110)//Si(110) (at $\chi=90°,\phi=0°$) (2) $FeSi_2$(100)//Si(001) and $FeSi_2$(110)//Si(011) (at $\chi=45°,\phi=45°$) (3) $FeSi_2$(111)//Si(001) and $FeSi_2$(110)//Si(110) (at $\chi=90°,\phi=0°$), and (4) $FeSi_2$(214)//Si(001) and $FeSi_2$(110)//Si(011) (at $\chi=45°,\phi=45°$) [Fig. 10].

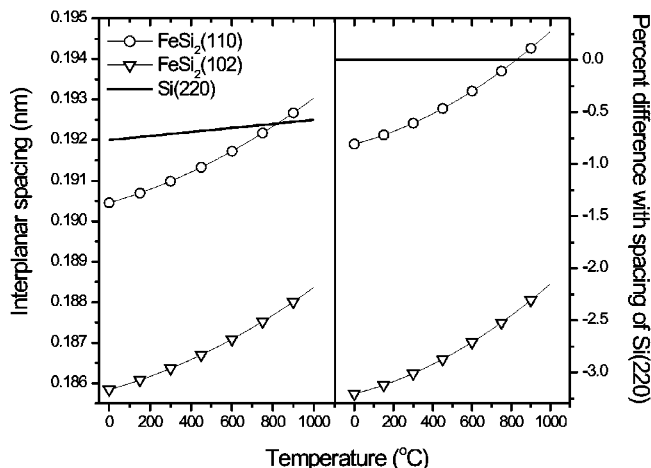

FIG. 8. The interplanar spacing for Si(220) and α-$FeSi_2$(110) and (102) planes as a function of temperature (left). The difference in interplanar spacing between the α-$FeSi_2$ planes and Si(220) is shown on the right.

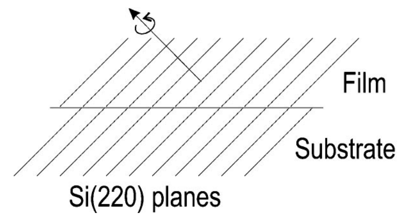

FIG. 9. Schematic illustration of the periodic interface structure that is achieved along one direction of the interface when two planes with the same interplanar spacing [the Si(220) and α-$FeSi_2$(110) planes] are aligned.

All four types of epitaxy have a low-index $FeSi_2$ plane parallel to the surface of the film, and a $FeSi_2\langle 110\rangle$ plane parallel to Si$\langle 110\rangle$. At first sight, one could argue that the bright spots on the lines are created whenever the rotation around the fiber axis positions a grain in a situation whereby a low-index $FeSi_2$ plane is parallel to the surface. However, this assertion is too general, since several low-index planes that could be parallel to the surface are missing from the above list [e.g., the $FeSi_2$(214) plane is present, while the (201) and (112) planes are missing].

It may be noted that some of the bright spots are located near points on the pole figure where different lines are crossing. It could therefore be argued that the bright spots are somehow related to the crossover points of different lines. This would actually be equivalent to the assumption that intense spots are caused by a situation whereby two different axiotaxy-type alignments occur within the same grain. For instance, one could imagine a situation whereby the $FeSi_2$(110) plane is parallel to Si(110), while the $FeSi_2$ (-110) plane in the same grain is parallel to Si(101). However, in order for such a situation to occur, it should be geometrically possible. As an example, it is impossible for a cubic grain to have its (100) plane at ($\chi=90°$, $\phi=0°$) and its (010) plane at ($\chi=90°$, $\phi=45°$) since the angle between the (100) and (010) planes in a cubic unit cell is 90°. Similarly, it can be verified that the above example for $FeSi_2$ is geometrically impossible for the tetragonal $FeSi_2$ unit cell. In fact, it can be verified that not a single crossing point exists between two bright lines (i.e., both lines caused by $FeSi_2\langle 110\rangle$//Si$\langle 110\rangle$) which corresponds to a situation whereby two poles for the same grain are located at a crossing point.

However, the idea that the bright spots are somehow related to points where lines are crossing should not be discarded altogether. Comparing the two sets of fitted lines on the pole figures (Figs. 4–6) makes it clear that most of the intense spots are actually located at crossing points between the bright $FeSi_2\langle 110\rangle$-related axiotaxy lines and the weaker $FeSi_2\langle 102\rangle$-related lines. These crossing points correspond to a situation whereby a $FeSi_2$(110)-type and a $FeSi_2$(102)-type plane are both parallel to a Si(110)-type plane within the same grain. For instance, the first type of epitaxial alignment from the above list [with $FeSi_2$(001)//Si(001)] corresponds to a situation whereby $FeSi_2$(110)//Si(-110) (at $\chi=90°,\phi=0°$) and $FeSi_2$(102)//Si(-101) (at $\chi\approx 45°,\phi=-45°$). A similar

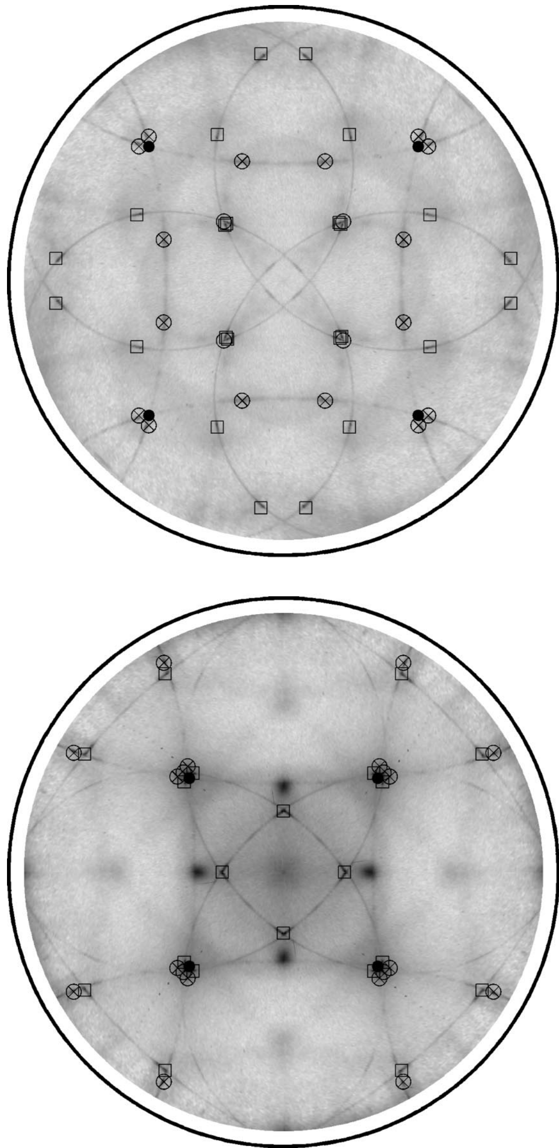

FIG. 10. The (101) (top) and (102) (bottom) pole figures, with the calculated locations of several epitaxial components overlaid on top of the measurement. All calculated poles are for grains with $FeSi_2\langle 110\rangle//Si\langle 110\rangle$ [either at ($\chi=90°,\phi=0°$) or ($\chi=45°,\chi=45°$)]. An epitaxial alignment is then defined by fixing the pole of a second plane. Poles labeled ● refer to grains for which $FeSi_2(001)//Si(001)$ (i.e., parallel to the surface), ○ indicates $FeSi_2(100)//Si(001)$ (or $FeSi_2(010)//Si(001)$), ⊗ indicates $FeSi_2(111)//Si(001)$, and □ indicates $FeSi_2(214)//Si(001)$ [or $FeSi_2(124)//Si(001)$].

type of situation occurs for the other epitaxial components, as illustrated in Table II. As a consequence of two independent types of axiotaxy being combined within the same grain, there are two independent directions within the plane of the interface [the Si(-110) and Si(-100) directions in the above example] along which a periodic interface structure is achieved. Since periodicity is achieved along two independent directions, the whole interface consists of a two-dimensional periodic structure, which leads to the interface "matching" well known for epitaxial alignment.

E. Interface structure

In order to be able to visualize the atomic structure at the interface for the different types of texture discussed in this paper, a computer program was developed that creates a three-dimensional model of the atomic structure (Fig. 11) near the interface region. The positions of the Fe ($x=y=z=0$) and Si atoms ($x=y=0.5$, $z=0.27$ or 0.73) in the $FeSi_2$ unit cell are taken from Ref. 17. For clarity, the Fe atoms are connected by lines, thus providing a view of the unit cell of the $FeSi_2$ lattice. The interface is visualized by viewing the three-dimensional structure from three different directions. The (a) view is along the Si(010) direction [i.e., at an angle of 45° with respect to the Si(110) cleaving direction]. The rows of Si atoms that make a 45° angle with the interface are Si(101) and Si(−101) planes. The (b) view is along the Si(−100) direction. The rows of Si atoms that make a 45° angle with the interface are the Si(011) and Si(−011) planes. The (c) view is along the Si(001) direction, i.e., looking down onto the sample. Since conventional XRD can only provide us with information regarding the orientation of planes in the film with respect to the substrate, it cannot be claimed that the pictures in Fig. 11 contain all details of the real interface structure, because there is no experimental information regarding the three degrees of freedom for translation or possible interface reconstruction. However, the interface models that are shown in this paper are helpful in visualizing the periodicity of the interface along certain directions.

In Fig. 11, we show the calculated interface structure for three different grains. The orientation of each of the grains is defined by choosing the location of two different poles. The first grain (poles indicated by ○) is located next to a line, in a region of the pole figure with low diffracted intensity, and clearly represents a "random" interface. The second grain (poles indicated by +) has its (101) pole located in a section of the line with low diffracted intensity, and represents the case of pure axiotaxy. In the (a) view, one observes alignment between the Si(101) planes and the $FeSi_2(110)$-type planes. However, neither the (b) nor (c) views of the same interface structure reveal any clear alignment between film and substrate. A similar observation was made for other dim points on the lines of the pole figure: the interface structure is only periodic along a single direction, and looks irregular when viewed from other angles. The third grain (poles indicated by x) has a (101) pole located in a section of the line with a high diffracted intensity. In this case, all three views of the interface structure reveal an alignment between film and substrate, indicating an epitaxial alignment. Figure 12 shows the interface structure models for all four types of epitaxial alignment that were shown to cause the bright spots on the lines. For all four cases, one observes periodicity along two independent directions within the plane of the interface.

IV. CONCLUSION

It is generally known that a geometrical "match" between the positions of the atoms in the film and substrate at the interface results in a significantly lower interfacial energy

TABLE II. Overview of geometrically allowed cases of double axiotaxy, i.e., where two planes within the same α-$FeSi_2$ grain are aligned with two different Si(110)-type planes. We considered all possible combinations of α-$FeSi_2$(102), (012), and (110) planes with their pole positioned at ($\chi=45°$; $\phi=45°,135°,225°,315°$) (*A*) or at ($\chi=90°$; $\phi=0,90°,180°,270°$) (*B*). If a given combination is geometrically possible, the α-$FeSi_2$ plane which is parallel to the Si(001) substrate is listed.

		102 *A*	102 *B*	012 *A*	012 *B*	110 *A*	110 *B*
102	*A*	001		001/111	100/124	100/124	001/111
102	*B*			010/214		010/214	
012	*A*	001/111	010/214	001		010/214	001/111
012	*B*	100/124				100/124	
110	*A*	100/124	010/214	010/214	100/124	100/010	
110	*B*	001/111		001/111			001

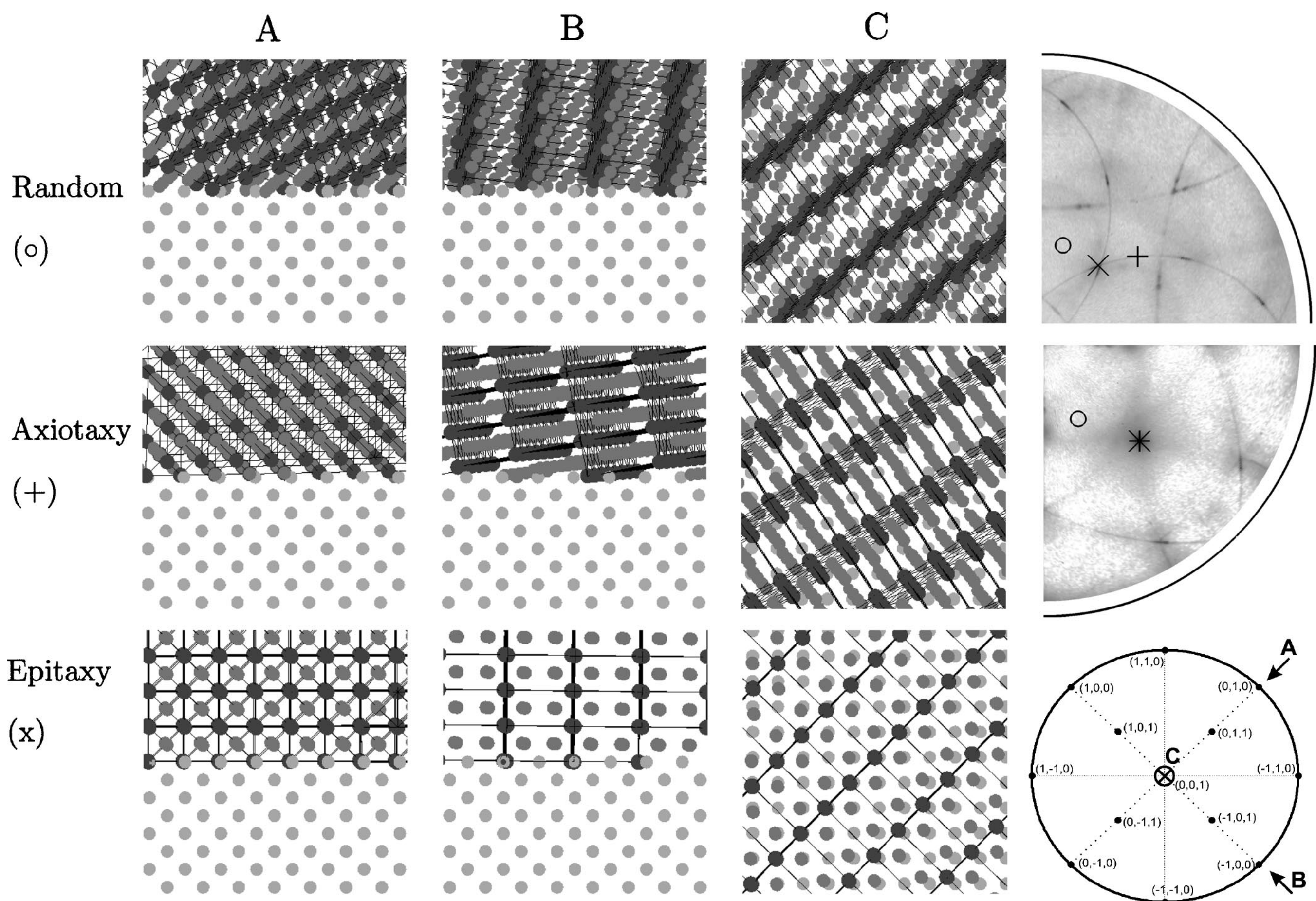

FIG. 11. Calculated interface structures for three $FeSi_2$ grains. The Fe atoms are shown as black dots. The orientation of the grains is defined by two points on the (101) (top) and (110) (bottom) pole figures. The top row of interface structures is for a random grain, with its poles (labeled ○) located in a region of the pole figure with low diffracted intensity. The middle row of interface structures is for a low-intensity point on one of the lines on the (101) pole figure (labeled + on the pole figures), while the bottom row of interface structures is for an intense spot on the same line (poles labeled *x*). The interface structures are viewed from three different directions, as indicated on the bottom pole figure, which also includes labels for the location of the Si substrate poles. The (a) view (left) is along the Si(010) direction [i.e., at an angle of 45° with respect to the Si(110) cleaving direction]. The (b) view (middle) is along the Si(-100) direction and the (c) view (right) is along the Si(001) direction, looking down onto the sample.

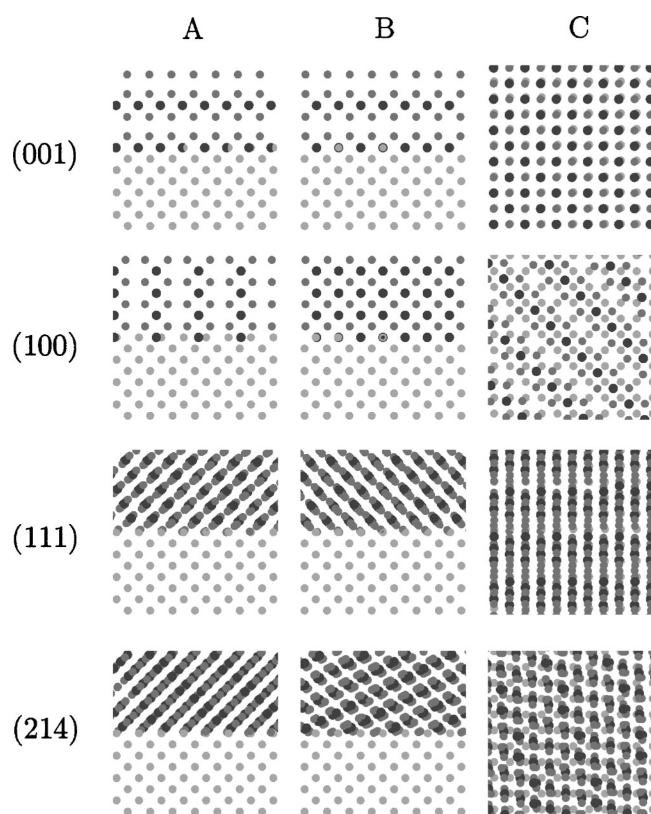

FIG. 12. Calculated interface structures for different kinds of epitaxy that correspond to bright spots along the lines on the pole figures. All calculated structures are for grains with $FeSi_2\langle 110\rangle//Si\langle 110\rangle$ [either at $(\chi=90°, \phi=0°)$ or $(\chi=45°, \phi=45°)$]. The epitaxial alignment is then defined by fixing the pole of a second plane: $FeSi_2(001)//Si(001)$ (top), $FeSi_2(100)//Si(001)$ (second row), $FeSi_2(111)//Si(001)$ (third row), and $FeSi_2(214)//Si(001)$ (bottom row). The interface structures are viewed from three different directions. The (A) view (left) is along the Si(010) direction. The (B) view (middle) is along the Si(-100) direction and the (C) view (right) is along the Si(001) direction, looking down onto the sample.

than for a random interface. The atomic structure of what is traditionally considered a matching interface will exhibit a two-dimensional periodic structure in the plane of the interface. On the basis of the measurements reported in this work, one may conclude that an intermediate situation can occur whereby a periodic arrangement of lattice planes exists along just a single direction in the plane of the interface. Although the interfacial energy for this intermediate case is bigger than for an epitaxial interface, the interfacial energy appears to be significantly smaller than for a random interface.

Periodicity along one direction in the plane of the interface can be achieved by the constraint that a low-index plane in the film that has the same interplanar spacing as a low-index plane in the substrate is fixed parallel to that substrate plane. Therefore, the texture manifests itself as an off-normal fiber texture. This situation has been named axiotaxy, and results in the formation of complex, though symmetrical line patterns on pole figures. Achieving a periodic structure along a second direction within the plane of the interface for a certain rotation around the fiber axis results in epitaxial alignment and is therefore expected to further reduce the interfacial energy. This explains the intensity variation along the lines on the pole figure. The brightest spots on the lines are interface structures for which epitaxial alignment is achieved.

Further work is needed to determine whether axiotaxy and the related concept of plane alignment (which were developed here to describe the interface between a polycrystalline film and a single-crystal substrate) can also be applied to grain boundaries in bulk materials. It is well known that "special" high angle grain boundaries exist, whereby the grain boundary energy is low because of a good match of the crystal lattice across the grain boundary. The quality of the match may be evaluated using the coincident site lattice. In fact, this "good match" also implies a periodic structure along two independent directions in the plane of the grain boundary, in analogy to the case of epitaxial alignment in thin films on a single-crystal substrate. For the case of possible axiotaxy at grain boundaries within a polycrystalline sample, one does not expect to observe any line patterns on pole figures, since there is no single-crystalline substrate that acts as a fixed frame of reference. However, when comparing the grain-to-grain orientation relationships, one would expect to see a similar decrease in grain-boundary energy whenever the structure of the grain boundary is periodic along just a single direction within the plane of the grain boundary.

ACKNOWLEDGMENTS

The synchrotron XRD experiments were conducted under U.S. DOE Contract No. DE-AC02-76CH-00016. The authors acknowledge R. Carruthers for sputter deposition. C. Detavernier thanks the Fonds voor Wetenschappelijk Onderzoek—Vlaanderen (FWO) for financial support. The authors are indebted to F. M. d'Heurle, J. M. E. Harper, K. Ludwig, C. Noyan, K. P. Rodbell, and F. M. Ross for interesting discussions.

*Also at Department of Solid State Physics, Ghent University, Gent, Belgium. Electronic address: christophe. detavernier@ugent. be

[1] U.F. Kocks, C.N. Tome, and H.-R. Wenk, *Texture and Anisotropy: Preferred Orientations in Polycrystals and their Effect on Materials Properties* (Cambridge University Press, Cambridge, 1976).
[2] V. Randle and O. Engler, *Introduction to Texture Analysis* (Gordon and Breach Science, New York, 2000).
[3] H.J. Bunge, *Texture Analysis in Materials Science—Mathematical Methods*, 2nd ed. (Butterworths, London, 1982).
[4] V. Nokinov, *Grain Growth and Control of Microstructure and Texture in Polycrystalline Materials* (CRC Press, Boca Raton, 1997).
[5] C.E. Murray and K.P. Rodbell, J. Appl. Phys. **89**, 2337 (2001).
[6] C.V. Thompson and R. Carel, Mater. Sci. Eng., B **32**, 217 (1995).
[7] J.M.E. Harper and K.P. Rodbell, J. Vac. Sci. Technol. B **15**, 763 (1997).

[8] C. Detavernier, A.S. Özcan, J. Jordan-Sweet, E.A. Stach, J. Tersoff, F.M. Ross, and C. Lavoie, Nature (London) **426**, 641 (2003).
[9] C.W.T. Bulle-Lieuwma, A.H. van Ommen, J. Hornstra, and C.N.A.M. Aussems, J. Appl. Phys. **71**, 2211 (1992).
[10] A.S. Özcan, K.F. Ludwig, Jr., P. Rebbi, C. Lavoie, C. Cabral, Jr., and J.M.E. Harper, J. Appl. Phys. **92**, 5011 (2002).
[11] A.S. Özcan, K.F. Ludwig, Jr., C. Lavoie, C. Cabral, Jr., and J.M.E. Harper, J. Appl. Phys. **92**, 7210 (2002).
[12] J.Y. Natoli, I. Berbezier, A. Ronda, and J. Derrien, J. Cryst. Growth **146**, 444 (1995).
[13] H.U. Nissen, E. Mueller, H.R. Deller, and H. von Kaenel, Phys. Status Solidi A **150**, 395 (1995).
[14] J. Derrien, I. Berbezier, A. Ronda, and J.Y. Natoli, Appl. Surf. Sci. **92**, 311 (1996).
[15] I. Berbezier, J. Chevrier, and J. Derrien, Surf. Sci. **315**, 27 (1994).
[16] Joint Committee on Powder Diffraction Standards (JCPDS) 35-0822.
[17] *Pearson's Handbook of Crystallographic Data for Intermetallic Phases*, 2nd ed., edited by P. Villars and L.D. Calvert (ASM International, Ohio, 1991).